

Converting Wannier into Frenkel Excitons in an Inorganic/Organic Hybrid Semiconductor Nanostructure

S. Blumstengel, S. Sadofev, C. Xu, J. Puls, and F. Henneberger*

Institut für Physik, Humboldt-Universität zu Berlin, Newtonstraße 15, 12489 Berlin, Germany

(Received 26 April 2006; published 7 December 2006)

Electronic coupling between Wannier and Frenkel excitons in an inorganic/organic semiconductor hybrid structure is experimentally observed. Time-resolved photoluminescence and excitation spectroscopy directly demonstrate that electronic excitation energy can be transferred with an efficiency of up to 50% from an inorganic ZnO quantum well to an organic [2,2-*p*-phenylenebis-(5-phenyloxazol), α -sexithiophene] overlayer. The coupling is mediated via dipole-dipole-interaction analog to the Förster transfer in donor-acceptor systems.

DOI: 10.1103/PhysRevLett.97.237401

PACS numbers: 78.66.Qn, 68.55.Ac, 78.67.Pt, 81.07.Pr

The exciton is the fundamental optical excitation of a dielectric solid. Nature has created two types of excitons. In materials, used in today's semiconductor technology, so-called Wannier excitons [1] are formed. Here, the relative motion of the electron and hole constituting the exciton encompasses hundreds of unit cells. In contrast, for the small-sized Frenkel excitons [2] found in weakly bound molecular crystals, electron and hole are located on the same molecule. The different sizes generate quite different properties: Wannier excitons start to interact at relatively low densities giving rise to a zoo of many-particle effects associated with optical nonlinearity and laser action, whereas Frenkel excitons hardly see each other but produce huge signatures in the optical spectra. In the long history of excitons, these two cases have always been considered as being physically separate. We will show in this Letter that the progress in material fabrication over the last years makes it feasible to manufacture hybrid semiconductor structures in which Wannier and Frenkel excitons are electronically coupled to each other. It has been theoretically predicted that such coupled excitons will exhibit unique features benefiting from the specific advantages of the individual species [3] and open up an avenue to a new class of optoelectronic applications. Until now, a very recent study on a GaInN-polymer structure merely yielded indirect signatures for radiationless energy transfer conjectured from the temperature dependence of the emission yield [4].

In order to realize electronic coupling between Frenkel and Wannier excitons, a hybrid nanostructure is required which brings the excitons into close contact. A suitable design is a layered system: A semiconductor quantum well (QW) confines the electronic excitations close to the inorganic surface covered by an organic overlayer [Fig. 1(a)]. Typical inorganic semiconductors are covalent—often with ionic contribution—while the molecules in organic crystals are weakly bound by π - π and van der Waals interactions. The growth of hybrid structures thus faces two major challenges. First, the attachment of molecules at dangling bonds present at the inorganic semiconductor

surface will affect the ordering of the organic overlayer and ruin its crystalline quality. Second, the interface between the inorganic and organic part has to be of high purity and electronic perfection, as otherwise defect states will destroy the coupling between the excitons and prevent energy transfer. A third requirement, much easier to fulfill, is resonance between the exciton energies of the inorganic and organic material, assuring sufficiently strong coupling on time scales shorter than the radiative lifetimes.

For reasons that are detailed in the following, we have chosen the II-VI compound ZnO as inorganic component. The organic part consists of a thin layer of either α -sexithiophene (6T) or 2,2-*p*-phenylenebis-(5-phenyloxazol) (POPOP). The structures of these molecules are depicted in Figs. 1(b) and 1(c), respectively. The samples are prepared in a molecular beam epitaxy appara-

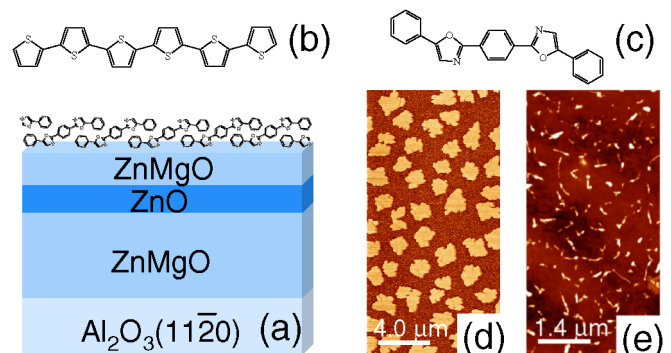


FIG. 1 (color online). (a) Sketch of the hybrid nanostructure. The 4 nm wide ZnO QW is situated on top of a 600 nm thick $\text{Zn}_{0.9}\text{Mg}_{0.1}\text{O}$ barrier layer grown on a $\text{Al}_2\text{O}_3(11\bar{2}0)$ substrate. The growth direction is along the wurtzite *c* axis. After capping with a $\text{Zn}_{0.9}\text{Mg}_{0.1}\text{O}$ spacer of variable thickness (0–50 nm), the sample is transferred into the adjacent chamber where the organic layer is deposited. (b),(c) Structures of 6T and POPOP. (d),(e) AFM images of 6T and POPOP deposited on $\text{ZnO}(0001)(4 \times 4)$ at a substrate temperature of 100 °C (6T) and 25 °C (POPOP), respectively, and a deposition rate of 1 Å/min.

tus equipped with separate growth chambers for organic and inorganic materials. This ensures that the organic layer is grown on a clean epitaxial surface without exposure to ambient atmosphere. 6T is a well-investigated molecular crystal and thus especially suited to analyze the structural and electronic properties of organic/ZnO interfaces. A typical atomic force microscopy (AFM) image of a 6T submonolayer deposited on epitaxial ZnO(0001) with a (4×4) surface reconstruction is shown in Fig. 1(d). The height of the 6T islands corresponds to the length of a 6T molecule. For an isolated molecule, it is energetically more favorable to lie flat on the surface. However, in crystals with a herringbone structure such as the 6T lattice, the (001) plane exhibits the lowest surface energy [5]. The 6T molecules should therefore orient upright in the islands, as exactly indicated by the experimental island height. It can thus be concluded that the intermolecular interactions out-balance the molecule-substrate interaction and that the molecules are bonded by van der Waals forces to the (0001) ZnO surface. X-ray photoelectron spectroscopy (XPS) confirms these conclusions and, in addition, substantiates that 6T is adsorbed electronically intact. Further experiments, not detailed here, have provided insight into the growth mechanisms. Nucleation of the 6T layer sets on immediately after start of the deposition and, as evident from the quite uniform lateral island size and separation in Fig. 1(d), is homogeneous in character. Self-similarity of the island morphology is observed when changing the substrate temperature, the incoming flux, or the surface coverage. The growth is thus diffusion mediated [6] and not disturbed by defects or dangling bonds of the ZnO surface. A similar growth scenario is observed for POPOP on ZnO(0001). Because of the arrangement of the POPOP molecules in the lattice [7], the preferred growth direction is along the b crystal axis resulting in layers constituted by needle-shaped crystallites [Fig. 1(e)]. Unlike other semiconductors, e.g., GaAs [8] or Si [9], no passivation of the ZnO(0001) surface is required to allow for an unperturbed ordered growth of the organic overlayer. The formation of chemically inert interfaces through stable bond reconstructions thus makes II-O materials especially well-suited candidates for the realization of electronically coupled organic/inorganic composites. A further motivation for the use of ZnO results from its large band gap of 3.37 eV and the resultant potential for the fabrication of light emitters in the visible and ultraviolet spectral range [10].

The inorganic ZnO/ZnMgO heterostructure is grown on a -plane sapphire; see Ref. [11] for details. A buffer layer, not shown in Fig. 1(a), is introduced in order to attain high crystalline quality. Proper annealing steps enable us to accomplish layer-by-layer growth and atomically flat interfaces for the ZnO QW with a thickness $L_{\text{QW}} = 4$ nm. A ZnMgO spacer of variable thickness L_S separates the QW from the organic layer on top of the structure. Both 6T and POPOP are capable of the energy transfer processes unveiled in what follows. However, owing to the considerably

brighter emission of POPOP, the spectroscopic signatures are much more pronounced here. POPOP is known for its intense blue fluorescence and, therefore, used as scintillator and laser dye [12].

Before dealing with the conversion of the inorganic and organic excitons, we specify relevant data for the separate subsystems obtained on appropriately shaped reference samples. Photoluminescence (PL) and PL excitation (PLE) spectra were measured at 5 K using a Xe lamp with the excitation wavelength selected by a double monochromator. The PL signals were recorded with a photomultiplier after passing a monochromator. Figure 2(a) compares the PL of the QW structure with the absorption (PLE) spectrum of POPOP. The latter shows a narrow band at 3.08 eV and a broader band at 3.29 eV due to the Frenkel-type transition followed by its vibronic replica. The narrow band is not present for the isolated molecule and assigned to a low-lying 1L_B state [13], optically allowed through conformational changes in the solid state. The Bohr radius of the Wannier exciton of bulk ZnO is 1.8 nm and the electron-hole binding energy 60 meV. A well width of $L_{\text{QW}} = 4$ nm assures in conjunction with the 240 meV band offset of the $\text{Zn}_{0.9}\text{Mg}_{0.1}\text{O}$ barriers robust carrier confinement. Prominent exciton emission from the QW and even laser action is indeed observed up to room temperature [11]. The fraction of photons absorbed by the well is

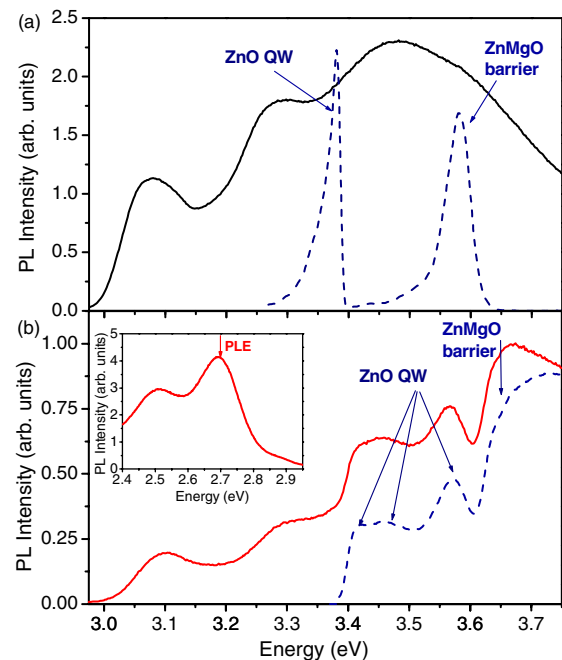


FIG. 2 (color online). (a) PLE spectrum of POPOP on Al_2O_3 (solid line) detected at the PL maximum and PL spectrum of a ZnO/ZnMgO QW structure ($L_S = 5.5$ nm) without organic overlayer (dashed line) under excitation in the barrier energy continuum. (b) PLE spectra of a POPOP/ZnO/ZnMgO hybrid structure with $L_S = 2.5$ nm recorded at the low-energy tail of the QW PL (dashed line) and at the maximum of the POPOP PL (solid line). The POPOP PL spectrum is displayed in the inset.

$A_{QW} \approx 0.1$, and its internal quantum efficiency η_{QW} approaches a value of 1 at 5 K. It is obvious from Fig. 2(a) that both the well and barrier Wannier excitons are degenerate in energy with the phonon replica of the organic Frenkel exciton.

Energy transfer in the hybrid structure is clearly revealed by PLE spectroscopy: Optical excitation in the absorption bands of the inorganic part gives rise to distinct signatures in the quantum yield of the POPOP emission. The PLE spectrum of the ZnO QW [dashed line in Fig. 2(b)] displays the band edge of the ZnMgO barriers as well as three exciton states of the QW itself related to the substructure of valence band edge of ZnO. Precisely these absorption features are prominently seen in the PLE of POPOP [solid line in Fig. 2(b)].

The time scale of the energy transfer between the inorganic QW and the organic overlayer is elaborated by time-resolved PL measurements. Figure 3 summarizes PL transients measured at 5 K by time-correlated single-photon counting with a resolution of 10 ps. The excitation pulses were delivered by the frequency doubled output of a synchronously pumped dye laser. Spectral selectivity is provided by a double monochromator in subtractive mode with a resolution of 0.4 nm. For a ZnO/ZnMgO QW without POPOP, the emission from the exciton ground-state decays in good approximation single exponentially with a time constant of $\tau_{QW} = 330$ ps [curve (i), Fig. 3(a)]. This value is in good agreement with the lifetime of the ZnO Wannier exciton of 322 ps [14]. In a hybrid structure with a thin spacer ($L_S = 2.5$ nm), the lifetime shortens to $\tau_{HB} = 160$ ps [curve (ii), Fig. 3(a)] confirming that an additional decay channel due to energy transfer opens up. Removing the POPOP overlayer by a proper solvent, the QW exciton recovers to the original decay time τ_{QW} . The PL transients of POPOP [inset of Fig. 3(a)] unambiguously verify that the excitation is indeed transferred to the organic overlayer: A rise time corresponding exactly to the lifetime τ_{HB} of the QW exciton, which is not present in the electronically passive POPOP/ Al_2O_3 specimen, emerges in the hybrid structure. Increasing the spacer thickness, the lifetime shortening quickly disappears. For a $L_S = 5.5$ nm spacer, the reduction is already less than 15% [Fig. 3(b)].

For a rectangular ZnO QW of the present width and band offset, we estimate a $1/e$ penetration depth of the carrier wave functions in growth direction of about 0.6 nm. The wave-function overlap with the organic part is thus negligible excluding tunneling processes or Coulomb exchange mediated coupling. A mechanism that does not require such overlap is given by the long-range dipole-dipole interaction. In this case, τ_{HB} should obey the specific dependence on the spacer length L_S derived in the following. Taking into account that the QW exciton is localized on interface fluctuations and/or alloy disorder, a treatment in the frame of the standard Förster theory [15] becomes reasonable. The dipole-dipole transfer rate is then given by

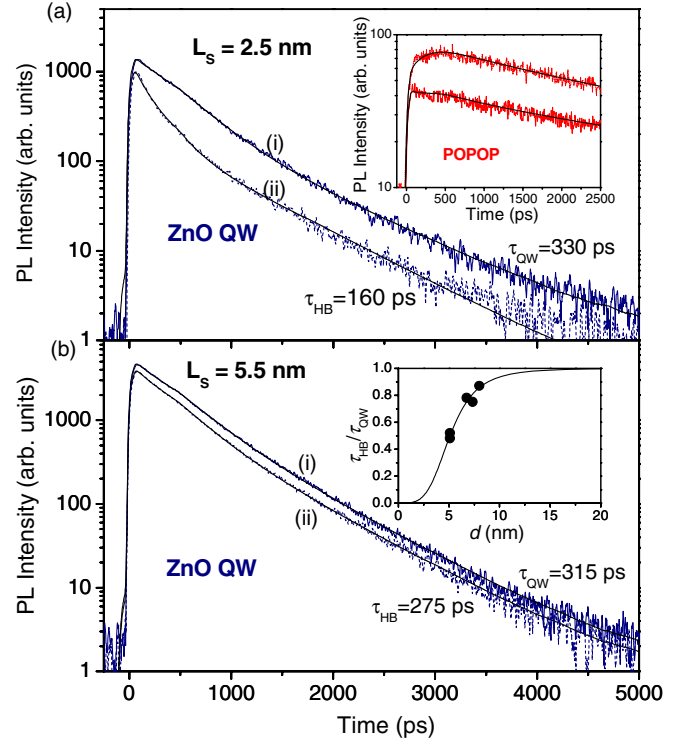


FIG. 3 (color online). PL transients of the ZnO QW in (i) a ZnO/ZnMgO reference sample and (ii) a POPOP/ZnO/ZnMgO hybrid structure: (a) $L_S = 2.5$ nm; (b) $L_S = 5.5$ nm. Convolution of the decay curves with the system response (solid lines) yields the Wannier exciton lifetimes τ_{HB} and τ_{QW} in the respective structure. A more than 10 times weaker slowly decaying background, occurring independently on POPOP deposition, is probably related to the capture of long-lived carriers from the ZnMgO barriers. Insets: (a) PL transients of POPOP on Al_2O_3 (lower curve) and in the hybrid structure of the main panel (upper curve). Solid lines are fits with a stretched exponential for the reference sample, while, in case of the hybrid, the raw data were convoluted with the system response and the QW decay curve demonstrating that the rise time corresponds to τ_{HB} . Excitation photon energy is 3.78 eV. (b) τ_{HB}/τ_{QW} versus distance d : •, experiment; solid line, theory (see text).

$1/\tau_{d-d} = (1/\tau_{QW})(R_0/R)^6$, where R is the donor-acceptor separation and R_0 the Förster radius. To obtain the total rate in the present geometry, one has to calculate the average over all the acceptor configurations for a plane with distance d from the donor layer. This yields for the PL transients $I(t) \sim \exp\{-\eta - N_0[(e^{-\nu^6 \eta} - 1)/\nu^2 + \eta^{1/3} \Gamma(\nu^6 \eta, 2/3)]\}$, $\eta = t/\tau_{QW}$, $\nu = R_0/d$. N_0 is the number of molecules in the Förster circle πR_0^2 , Γ refers to the incomplete Gamma function, and $d = L_S + L_{QW}/2$. As the decay is nonexponential, we define the lifetime by $\tau_{HB} = \int dt t I(t) / \int dt I(t)$. In the inset of Fig. 3(b), the ratio τ_{HB}/τ_{QW} deduced from the experimental transients is plotted versus d for five different hybrid structures together with a fit using the above model. Assuming a sheet density of $1.4 \times 10^{14} \text{ cm}^{-2}$ of the POPOP molecules [16], the best agreement is found for $R_0 = 2.6$ nm. On the other hand,

the Förster radius R_0 can also be calculated from spectroscopic quantities by $R_0^6 = \frac{3\eta_{\text{QW}}}{2(2\pi)^5 N_p n^4} \times \int \frac{f_{\text{QW}}(\tilde{\nu})\alpha_{\text{PP}}(\tilde{\nu})}{(\tilde{\nu})^4} d\tilde{\nu}$ [15]. The spectral overlap between the normalized line-shape function of the QW emission (f_{QW}) and the POPOP absorption coefficient [$\alpha_{\text{PP}}(3.38 \text{ eV}) \approx 2 \times 10^5 \text{ cm}^{-1}$] is easily computed from the spectra in Fig. 2(a). Using for the POPOP volume density $N_p = 2.1 \times 10^{21} \text{ cm}^{-3}$ [7] and $n = 2$ for the refractive index of ZnMgO, it follows $R_0 \approx 3.5 \text{ nm}$. In view of the uncertainties in the parameters, the results of both approaches are in fair agreement.

Attempts to reach still shorter transfer times by using thinner spacers were not successful as the PL from the QW became increasingly quenched. At $L_S = 10 \text{ nm}$, Frenkel and Wannier excitons are practically electronically isolated. Nonetheless, energy transfer between the QW and the organic layer is still observed at separations far beyond the Förster radius. We have found clear signatures even for $L_S = 50 \text{ nm}$, the largest spacers used so far. However, no shortening of the lifetime occurs here. At those length scales, the Förster mechanism turns into radiative transfer where the excitonic emission from the QW is reabsorbed by the organic overlayer. Denoting the density of Frenkel excitons generated in a sole molecular layer and in the hybrid structure by n_0 and n_{HB} , respectively, under identical optical excitation, the strength of the energy transfer can be characterized by the ratio $Q = (n_{\text{HB}} - n_0)/n_0$. Neglecting a difference in the absorption of the incident photons and those emitted from the QW by the organic overlayer, it is straightforward to show that $Q_{\text{RT}} = q\eta_{\text{QW}}A_{\text{QW}}$ holds for radiative transfer. $q < 1/2$ is a geometry parameter accounting for the part of light emitted by the QW which penetrates the organic layer. An upper limit is thus $Q_{\text{RT}} = 0.05$ ($A_{\text{QW}} = 0.1$, $\eta_{\text{QW}} = 1$). The PLE data in the dipole-dipole regime of Fig. 2(b) yield about one order of magnitude larger values for Q , demonstrating the considerably stronger efficiency of the Förster transfer.

The above results elucidate several important aspects of inorganic/organic hybrid nanostructures. Interfaces of high structural and electronic perfection can indeed be assembled by molecular beam epitaxy. Organic overlayers deposited on top of the ZnO surface grow in a well-defined mode without the need of extra passivation layers that would reduce the electronic coupling. Dipole-dipole coupling between Frenkel and Wannier excitons is accomplished only in a limited window of spacer lengths. There is a trade-off between the cap thickness required to form QWs of sufficient quality and the length scale on which the dipole-dipole interaction is efficient. The energy transfer is of the Förster type, similarly as in molecular donor-acceptor systems, and the highest efficiency achieved in the tested hybrid structures is $\eta_{\text{ET}} = \tau_{\text{QW}}/(\tau_{\text{QW}} + \tau_{d-d}) = 0.5$. Comparable efficiencies have been recently reported for the dipole-dipole mediated injection of free carriers from an InGaN QW into CdSe

nanocrystals [17]. The optically pumped carrier densities are, however, orders of magnitude larger than in our inorganic/organic hybrid system.

The present work is a proof-of-concept study. While electronic coupling of Wannier and Frenkel excitons is principally demonstrated, there is still space for improvement. Energy transfer is observed up to about 100 K. The presence of nonradiative centers and their activation at higher temperatures shortens the exciton lifetimes and decreases the transfer efficiency. The use of different designs, e.g., with binary barriers in the inorganic part, can be a solution to this problem. In this Letter, we have restricted the presentation on 6T and POPOP; however, we have found the same type of energy transfer for various other molecules (spiro-linked hexaphenyl, fluorene/carbazole co-oligomer). More systematic studies of the coupling mechanism are necessary in order to optimize the length dimensions in the hybrid structure and to increase the coupling strength. The simple donor-acceptor model provides a correct order-of-magnitude estimate; however, the exact geometry and wave functions are certainly of relevance. Our findings also represent a starting point for the construction of true hybrid excitons. For this goal, other organic molecules have to be chosen, as the spectral linewidth of the POPOP Frenkel exciton is much too large to enable coherent coupling.

We acknowledge the financial support of the Deutsche Forschungsgemeinschaft within the frame of Sfb 448. We also thank N. Koch for the XPS measurements.

*Electronic address: fh@physik.hu-berlin.de

- [1] G. H. Wannier, Phys. Rev. **52**, 191 (1937).
- [2] J. Frenkel, Phys. Rev. **37**, 17 (1931).
- [3] V. M. Agranovich, D. M. Basko, G. C. La Rocca, and F. Bassani, J. Phys. Condens. Matter **10**, 9369 (1998).
- [4] G. Heliotis *et al.*, Adv. Mater. **18**, 334 (2006).
- [5] J. E. Northrup, M. L. Tiago, and S. G. Louie, Phys. Rev. B **66**, 121404 (2002).
- [6] T. Vicsek, *Fractal Growth Phenomena* (World Scientific, Singapore, 1992).
- [7] I. Ambats and R. E. Marsh, Acta Crystallogr. **19**, 942 (1965).
- [8] Y. Hirose, S. R. Forrest, and A. Kahn, Phys. Rev. B **52**, 14040 (1995).
- [9] G. Hughes *et al.*, J. Vac. Sci. Technol. B **20**, 1620 (2002).
- [10] A. Tsukazaki *et al.*, Nat. Mater. **4**, 42 (2005).
- [11] S. Sadofev *et al.*, Appl. Phys. Lett. **87**, 091903 (2005); Jian Cui *et al.*, Appl. Phys. Lett. **89**, 051108 (2006).
- [12] P. W. Smith *et al.*, IEEE J. Quantum Electron. **11**, 84 (1975).
- [13] A. K. Dutta, J. Phys. Chem. B **101**, 569 (1997).
- [14] D. C. Reynolds *et al.*, J. Appl. Phys. **88**, 2152 (2000).
- [15] See, e.g., V. M. Agranovich and M. D. Galanin, *Electronic Excitation Transfer in Condensed Matter* (North-Holland, Amsterdam, 1982).
- [16] D.-M. Smilgies *et al.*, J. Cryst. Growth **220**, 88 (2000).
- [17] M. A. Achermann *et al.*, Nature (London) **429**, 642 (2004).